Compact Circularly Polarized Wearable Button Antenna with Broadside Pattern for U-NII Worldwide Band Applications

Xiaomu Hu, Sen Yan, and Guy A. E. Vandenbosch

***Abstract*—A novel circularly polarized button antenna is proposed. The antenna is constructed on a disc shaped FR-4 substrate. This disc is located on top of a textile layer and supported by a feeding probe. The antenna works in the 5.47-5.725 GHz U-NII world wide band, with over 14% relative impedance bandwidth and over 7% relative axial ratio bandwidth. A prototype has been fabricated and measured. A good agreement is found between measured and simulated results.**

***Key words*—Circular polarization, Axial ratio, Wearable, Button antenna, U-NII band.**

I. Introduction

The past decade saw an increasing research interest in body-centric wireless devices [1-7]. Research has been performed in numerous areas, such as health monitoring [6], indoor body-centric communication [3,7], radio frequency identification, on-body GPS location, etc. However, the polarization mismatch issue of wearable antennas has been scarcely touched upon. While already being an issue in handheld terminal communications [8], the polarization loss factor could be further amplified by human body movements for these antennas, causing challenges in communication quality. A feasible solution regarding this issue is to design a circularly polarized wearable antenna rather than a linearly polarized antenna. Over the years, several articles have addressed this method for different applications [9-17]. Most of these papers focus on the 2.4GHz ISM band, with a flexible design to fit on the human body [11-14]. On the other hand, circularly polarized antennas aiming at 5GHz or higher are less focused on, with even fewer efforts to make this idea fit into body-centric applications [16]. With indoor wireless communication moving into the higher frequency band for better channel capacity and transmission speed, more attention should be paid to this issue.

In this work, a novel circularly polarized button antenna is proposed, covering the 5.47-5.725GHz U-NII worldwide band. The main radiator was designed and built on a rigid FR-4 substrate in the shape of a small button, with a flexible matching circuit on the surface of the textile layer. The antenna also features a relatively compact size and a broadside radiation pattern and is especially suited for on-torso off-body channel applications. However, if bending is allowed, on-arm topologies are also possible. The antenna successfully achieves the targeted impedance and AR bandwidth, with a relatively high radiation efficiency. In Table I, a performance comparison is given between the proposed antenna and similar antennas in literature. Note that since the flexible ground in our antenna is of a textile nature and in practice can thus be implemented as part of the garment, the size of the ground is not a real issue during the integration of the antenna, and thus larger ground plane sizes are allowed. The real challenge is to reach the specifications for the antenna with a button conform to existing button sizes. Therefore, the ka values of the actual radiators are compared in the table. The radiator of the topology in reference [11] is smaller in size. However, it is achieved with more expensive high-k materials as antenna substrate. If this model would use the much cheaper FR4 substrate instead (the same as used in our work), the ka value would increase to 2.07, which is much bigger than the 1.12 obtained in our work. As far as the authors can see, this is the only work featuring a wearable circularly polarized unidirectional button antenna within the 5GHz band. On top, the radiating structure of the antenna is one of the smallest of its kind and the antenna only uses a cheap and

Table I. Comparison with literature

Ref.	f_0 (GHz)	ka of radiator*	Height /Thickness (mm)	Impedance -10dB BW (GHz)	AR 3dB BW (GHz)	Button Antenna
[9]	1.6	1.42	7.7	1.5-1.7	1.5-1.7	No
[10]	1.6	1.53	3	1.59-1.67	1.61-1.65	No
[11]	2.2	0.81	1.3	2.15-2.49	2.1-2.3	No
[4]	2.45	1.77	3.5	2.37-2.64	2.4-2.47	No
[14]	2.45	1.36	7.7	2.39-2.44	2.42-2.47	No
[1]	2.45	1.73	3.94	2.33-2.58	2.4-2.46	No
[13]	2.45	1.85	1	1.94-3.03	2.16-2.66	No
[12]	2.45	Not mentioned	5.2	2.38-2.49	2.4-2.47	No
[15]	2.45	1.79	Not mentioned	2-3GHz	2.29-2.36	No
[16]	4	1.31	5.3	3.77-4.24	3.77-4.26	No
[17]	5.5	1.24	1.6	5.0-6.4	5.0-5.8	No
This work	5.5	1.12	12	5.42-6.10	5.44-5.8	Yes

***a is the radius of the disc enclosing the antenna's radiator**

Manuscript submitted on _____. This work was partly supported by Internal DOC Funds of the KU Leuven and the FWO Postdoctoral Fellowship No. 12O1217N. *(Corresponding author: Sen Yan.)*

X. Hu and G.A. E. Vandenbosch are with TELEMIC, Department of Electrical Engineering, KU Leuven, Leuven 3001, Belgium (E-mail: hxiaomu@esat.kuleuven.be).

S. Yan is with the School of Electronics and Information Engineering, Xi'an Jiaotong University, Xi'an, Shanxi 710049, China, and also with TELEMIC, Department of Electrical Engineering, KU Leuven, Leuven 3001, Belgium. (E-mail: sen.yan@xjtu.edu.cn)

Color versions of one or more of the figures in this paper are available online at http://ieeexplore.ieee.org.

doi:

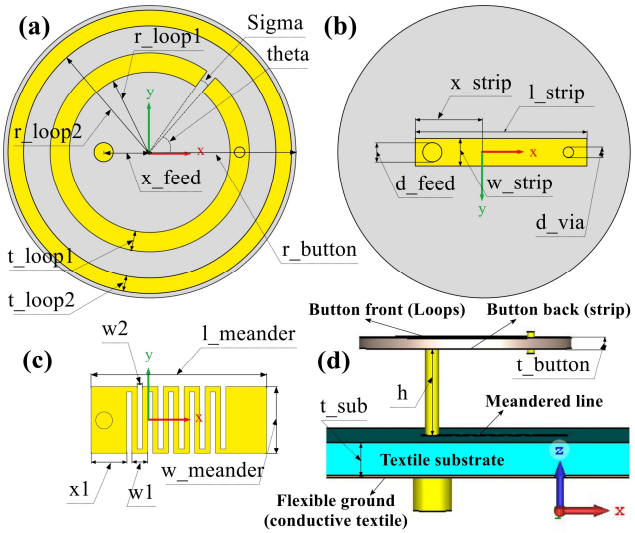

Fig. 1. Antenna Configuration. (a) Front view of the button. (b) Back view of the button. (c) Geometry of the meandered line. (d) Side view.

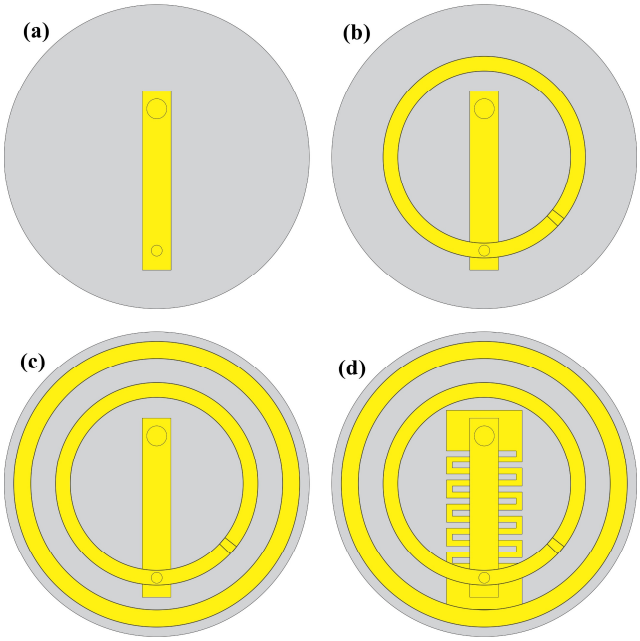

Fig. 2. The four steps of the antenna design: (a) probe fed strip with loading, (b) with the gap loaded loop, (c) with the outer enhancing loop, (d) with the meandered line for impedance matching.

common substrate.

CST Microwave studio 2016 was used in the design and simulation phase [18]. Measurements were performed using an Agilent Vector Network Analyzer and the anechoic chamber at KU Leuven.

II. Topology

In Fig. 1, the topology of the proposed circularly polarized button antenna is presented. The main body of the antenna is constructed on a button shaped FR-4 substrate (thickness of 1mm, permittivity of 4.3, loss tangent of 0.025), with radiating elements on both sides. On the top surface of the button, a full metal circle and a smaller gapped metal circle are printed. On the button's bottom surface, a rectangular metal strip is present,

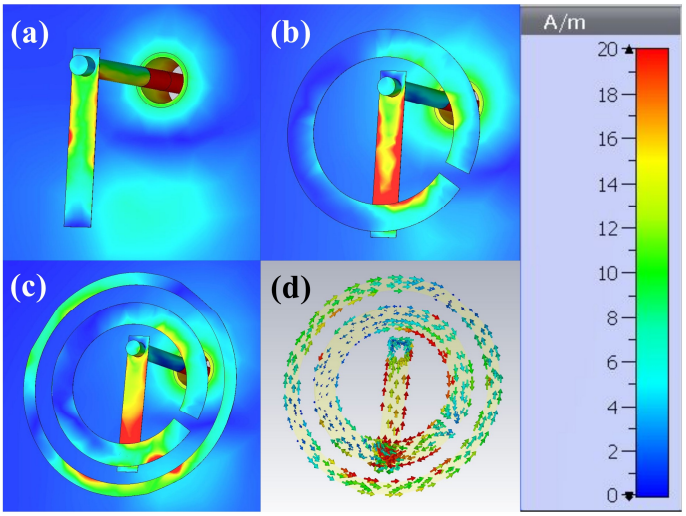

Fig. 3. Surface current distribution at 5.5 GHz: (a) single probe fed rectangular strip, (b) with gap loaded loop added, (c) with outer enhancing loop added. (d) direction of the surface current on strip and loops.

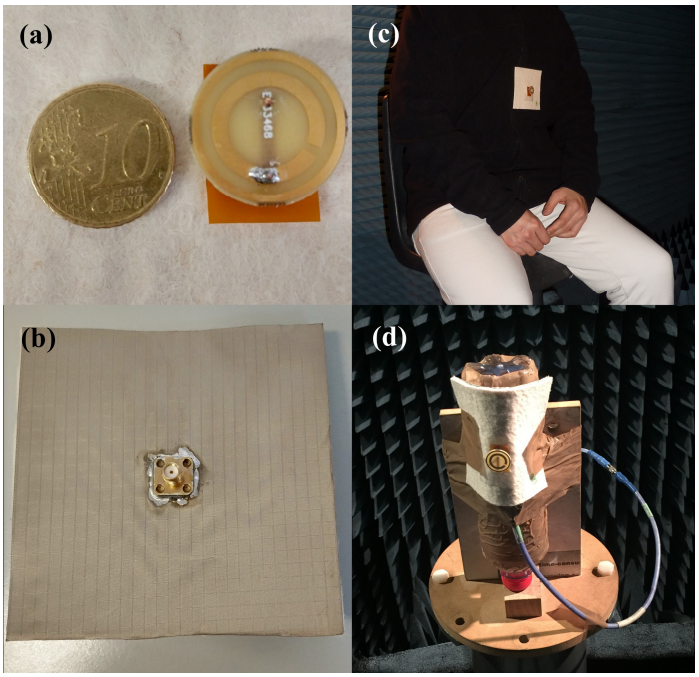

Fig. 4. (a) Fabricated prototype. (b) Backside view. (c) On-torso measurement setup. (d) Measurement setup with bending mimicking an on-arm situation.

Table II. Antenna parameters.

Parameter	Value	Parameter	Value
d_feed	1.28 mm	t_loop2	1.04 mm
d_via	0.70 mm	t_sub	3 mm
h	8 mm	theta	56.26 °
l_meander	13.44 mm	w_meander	5.11 mm
l_strip	11.47 mm	w_strip	1.84 mm
r_button	9.77 mm	w1	1.2 mm
r_loop1	5.07 mm	w2	0.4 mm
r_loop2	8.43 mm	x_feed	3.08 mm
sigma	9.57 °	x_strip	4.22 mm
t_button	1 mm	x1	2.73 mm
t_loop1	1.88 mm		

with a shorting pin on one end to the top-side's gapped loop. On the other end of the rectangular strip, a feeding probe is

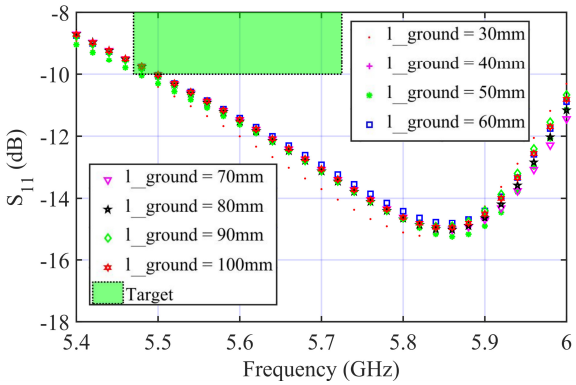

Fig. 5. Impact of different ground sizes on reflection coefficient performance

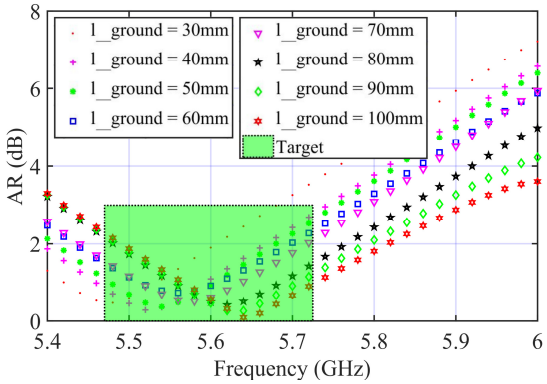

Fig. 6. Impact of different ground sizes on Axial Ratio performance

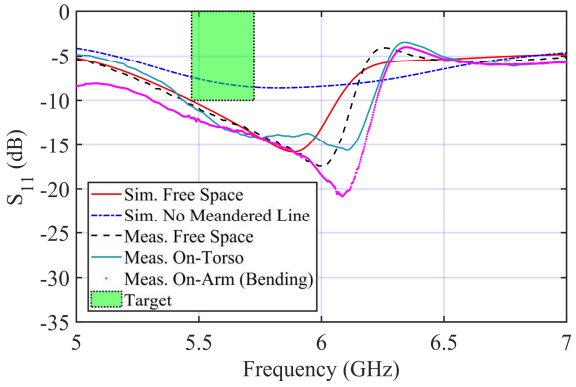

Fig. 7. Simulated and measured reflection coefficient. The free space case indicates that the complete antenna, including conducting textile ground, is mounted on a positioner in an anechoic room.

directly connected to the coaxial feed below the flexible conductive textile ground. The feeding probe also serves as support for the antenna's main body. At the lower part of the structure, there is a 3 mm thick layer of normal textile from RS components© that serves as the supporting substrate. Finally, a layer of conductive textile, SHIELDIT™ SUPER is found at the bottom of the whole structure forming the flexible ground, as shown in Fig. 4 (b). SHIELDIT is a material well-known for shielding purposes, but the latest few years, it has been also used a lot as conductor in textile antennas [19]. Both the normal and the conductive textile layer can be easily integrated into

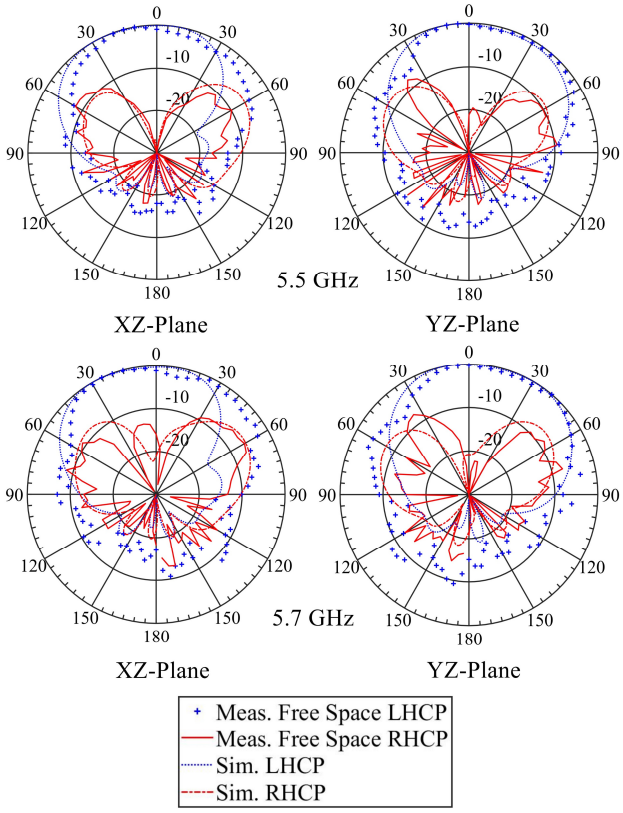

Fig. 8. Simulated and measured far-field patterns in free space at (a) 5.5GHz (b) 5.7GHz.

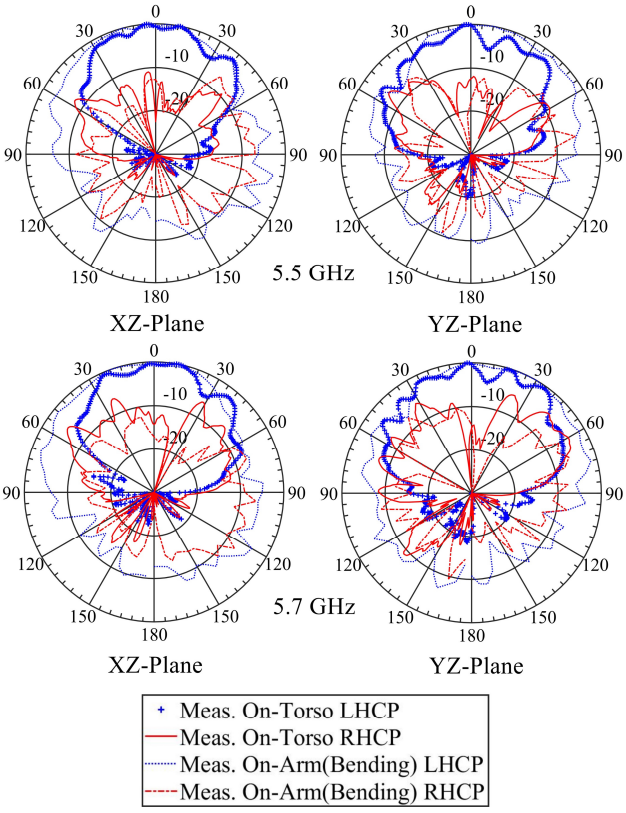

Fig. 9. Measured far-field patterns on-torso and on-arm (bending) at (a) 5.5GHz (b) 5.7GHz.

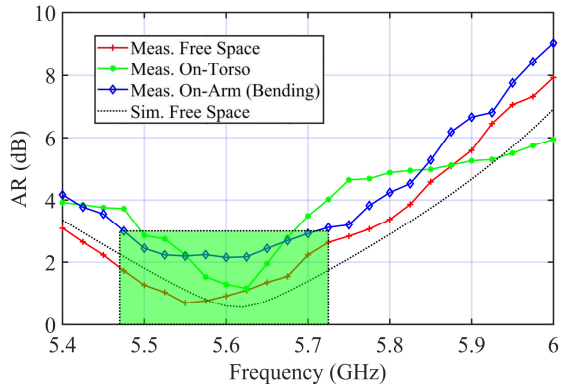

Fig. 10. Simulated and measured Axial Ratio in the broadside direction.

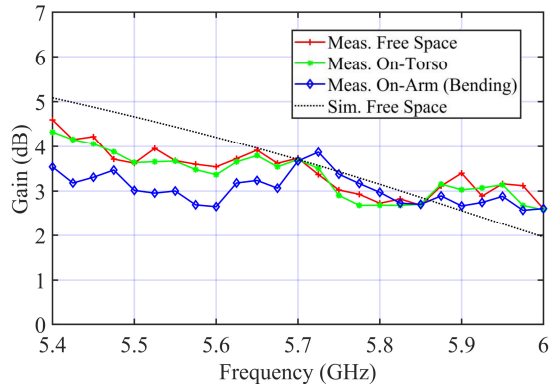

Fig. 11. Simulated and measured gain.

Table III. Performance of the antenna.

	Sim. Free Space	Meas. Free Space	Meas. On Arm	Meas. On Arm Bending
-10 dB Impedance Bandwidth (GHz)	**5.47-6.08**	**5.43-6.11**	**5.40-6.11**	**5.3-6.22**
3 dB Axial Ratio Bandwidth (GHz)	**5.42-5.80**	**<5.40-5.69**	**5.40-5.69**	**5.57-5.71**
Radiation Efficiency	**5.5GHz: 79.9%**		**5.7GHz: 75.7%**	
Total Efficiency	**5.5GHz: 71.5%**		**5.7GHz: 70.8%**	

human clothing. The permittivity and loss tangent of the textile are 1.4 and 0.044, and the conductivity of the conductive textile is 1.18×10^5 S/m. This conductivity is lower as in the case of copper, which typically leads to the lower efficiencies in textile antennas. The size of both the ground and the textile is 100mm × 100mm. The airgap between the button body and the textile substrate is 8mm. On top of the textile layer, a flexible PCB of 23mm × 16mm is placed, with a meandering line. The thicknesses of the textile layer and the conductive textile ground are 3mm and 0.17mm, respectively. In Table. II, the antenna parameters are given in detail.

III. Design Process and Operation

The main goal of this design is to achieve a compact wearable button antenna with circular polarization in the off-body direction. The design process can be divided into four steps. First, a broad-side pattern is obtained by loading a rectangular strip to the monopole-like feeding probe, see Fig. 2 (a). In this way, a linearly polarized antenna is achieved. To realize circular polarization, the complementary normal component must be generated. This is done with a gap loaded strip loop, see Fig. 2 (b). By carefully designing the loop, which can be seen as a magnetic dipole, and its gap, a quasi-circularly polarized pattern is obtained in the far-field. To further improve the axial ratio performance of the structure, a full loop outside the gap loaded loop is added to the structure, see Fig. 2. (c). Finally, an open meandered line is added to the structure, as shown in Fig. 2 (d), introducing inductive impedance matching.

The operational principle of the antenna is illustrated in Fig. 3. In Fig. 3 (a), the surface current of the single rectangular strip loaded monopole at 5.5GHz is presented. As can be observed, the current is mainly concentrated on the strip, leading to a broadside pattern. In Fig. 3 (b), the effect of the gap loaded loop is shown. A surface current lower than the strip current is distributed over the loop half where the gap is situated. Finally, the outer loop is added. The surface current shows a more densified distribution on the gap loaded and full loop, generating the correct component needed for the circular polarization, see Fig. 3 (c). In Fig. 3 (d), the direction of the surface current on strip and loops is shown. The current direction is consistent on the strip, indicating a dipole-like current distribution parallel to the ground, while the current direction on the loops are inconsistent, showing two opposite directions, indicating a multiple dipole-like distribution parallel to the ground. This explains the broadside far-field pattern seen in Fig. 8 and 9.

Note that the proposed antenna uses a large flexible conducting textile as ground. In Fig. 5 and 6, the impact of different ground sizes in free space is shown. It can be observed that the ground size does not have a large impact on the reflection coefficient performance. However, the point with the lowest AR shifts by approximately 200 MHz with the increase of the ground size from 30 mm to 100 mm. It is important to emphasize that the flexible ground in practice can be implemented as part of the garment, thus larger sizes are not a problem in real life. Taking this into consideration, a relatively large ground size of 100×100 mm^2 was chosen for the fabricated prototype.

IV. Results

A prototype of the antenna was fabricated and measured, see Fig. 4 (a). The on-torso measurement setup is shown in Fig. 4 (c). For the on-arm situation, a bottle of body simulating liquid MSL2450v2 was used to mimic a human arm, as shown in Fig. 4 (d). The bottle's radius is approximately 30mm. An SMA connector was used to feed the structure. The detailed performances of the proposed antenna are listed in Table III.

A. Reflection Coefficient and Radiation Pattern

The reflection coefficient is shown in Fig. 7. The model without meandered line does not reach -10dB, while the

simulated model with meandered line covers a bandwidth of over 610MHz, ranging from 5.47 to 6.08GHz. The measurements show a slightly wider -10 dB bandwidth, ranging from 5.43 to 6.11GHz. It is seen that the human body's presence does not have a large impact on the reflection coefficient, proving the effectiveness of the large ground plane. Remarkably, the on-arm (bending) situation results in a lower reflection in a wider band, which could be due to the combination of bending and losses.

In Fig. 8 and 9, the simulated and measured radiation patterns are given. The main polarization of the antenna is the left-handed circular polarization. It is clearly seen that the LHCP main beam direction and beam width are very well predicted and are maintained in all situations: free space, on torso, and even on arm. In the main beam the RHCP is always below –10dB. The backside radiation is in the order of -10dB. These numbers are common in wearable situations.

B. Axial Ratio

The axial ratio in the broadside direction is displayed in Fig. 10. The free space simulation result indicates a 3dB axial ratio bandwidth from 5.42GHz to 5.81GHz, covering the targeted bandwidth. The measurement in free space agrees well with the simulated results. The on-torso measurement shows a notably narrowed frequency bandwidth, from 5.49GHz to 5.69GHz. This could be caused by the inevitable small movement of the human body during the measurement. Finally, the on-arm (bending) situation shows a similar, but slightly shallower axial ratio curve compared to the free space result. The results also cover the targeted bandwidth, illustrating the robustness with respect to the ground curvature.

C. Gain

The simulated and measured gain are shown in Fig 11. A discrepancy of up to 2dBi is present in the lower frequency band. The measured results are relatively flat (around 3.5dBi) across the entire operating band. It is worth mentioning that in the on-arm (bending) situation the gain shows a similar effect as in the case of the axial ratio, with a shift in frequency of approximately 200MHz.

V. Conclusion

A novel circularly polarized button antenna for U-NII 5.47-5.725GHz applications was proposed, simulated, prototyped, and measured. The proposed antenna is the first button structure reaching circular polarization in this band, and this with a very compact size. The measured antenna performance agrees well with the simulated one.

References

[1] Carla Hertleer, Hendrik Rogier, Luigi Vallozzi, Lieva Van Langenhove, "A Textile Antenna for Off-Body Communication Integrated into Protective Clothing for Firefighters", IEEE Transactions on Antennas and Propagation, pp. 919-925, Volume 57, Issue 4, April 2009.

[2] Jiahao Zhang, Sen Yan, Guy A. E. Vandenbosch, "A Miniature Feeding Network for Aperture-Coupled Wearable Antennas", IEEE Transactions on Antennas and Propagation, Volume: 65, Issue: 5, pp. 2650-2654, Mar. 2017.

[3] Sen Yan, Guy A. E. Vandenbosch, "Radiation Pattern-Reconfigurable Wearable Antenna Based on Metamaterial Structure", IEEE Antennas and Wireless Propagation Letters, Volume: 15, pp. 1715-1718, Feb. 2016.

[4] Zhi Hao Jiang, Zheng Cui, Taiwei Yue, Yong Zhu, Douglas H. Werner, "Compact, Highly Efficient, and Fully Flexible Circularly Polarized Antenna Enabled by Silver Nanowires for Wireless Body-Area Networks", IEEE Transactions on Biomedical Circuits and Systems, pp. 920-932, Volume 11, Issue 4, May 2017.

[5] Hu Xiaomu, Sen Yan, Guy A. E. Vandenbosch, "Wearable Button Antenna for Dual-Band WLAN Applications with Combined on and off-Body Radiation Patterns", IEEE Transactions on Antennas and Propagation, Volume: 65, Issue: 3, pp. 1384-1387, Jan. 2017.

[6] Ping Jack Soh, Bertold Van den Bergh, Hantao Xu, Hadi Aliakbarian, Saeed Farsi, Purna Samal, Guy A. E Vandenbosch, Dominique M. M. -P. Schreurs, Bart K. J. C. Nauwelaers, "A smart wearable textile array system for biomedical telemetry applications", IEEE Transactions on Microwave Theory and Techniques, Volume: 61, Issue: 5, pp. 2253-2261, Feb. 2013.

[7] Linda A. Yimdjo Poffelie, Ping Jack Soh, Sen Yan, Guy A. E. Vandenbosch, "A High-Fidelity All-Textile UWB Antenna with Low Back Radiation for Off-Body WBAN Applications", IEEE Transactions on Antennas and Propagation, Volume: 64, Issue: 2, pp. 757-760, Dec. 2015.

[8] Carl B. Dietrich, Jr., Kai Dietze, J. Randall Nealy, and Warren L. Stutzman, "Spatial, Polarization, and Pattern Diversity for Wireless Handheld Terminals", IEEE Transactions on Antennas and Propagation, Volume: 49, Issue: 9, pp. 1271-1281, Sept. 2001.

[9] Arnaut Dierck, Hendrik Rogier, Frederick Declercq, "An active wearable dual-band antenna for GPS and Iridium satellite phone deployed in a rescue worker garment", RFID-Technologies and Applications (RFID-TA), 2013 IEEE International Conference on, pp. 1-5, Sept. 2013, Johor Bahru.

[10] Emmi K. Kaivanto, Markus Berg, Erkki Salonen, Peter de Maagt, "Wearable Circularly Polarized Antenna for Personal Satellite Communication and Navigation", IEEE Transactions on Antennas and Propagation, Volume: 59, Issue: 12, pp. 4490-4496, Dec. 2011.

[11] N. Ehteshami, V. Sathi, M. Ehteshami, "Experimental investigation of a circularly polarized flexible polymer-composite microstrip antenna for wearable applications", IET Microwaves, Antennas & Propagation, pp. 1681 – 1686, Issue 15, Dec. 2012.

[12] Zhi Hao Jiang, Micah D. Gregory, Douglas H. Werner, Pingjuan L. Werner, "A Compact Circularly Polarized Wearable Filtering Antenna for Off-Body Communications", 2015 9th European Conference on Antennas and Propagation (EuCAP), pp. 1-4, April 2015, Lisbon.

[13] K. W. Lui, O. H. Murphy, C. Toumazou, "A Wearable Wideband Circularly Polarized Textile Antenna for Effective Power Transmission on a Wirelessly-Powered Sensor Platform", IEEE Transactions on Antennas and Propagation, pp. 3873 – 3876, Volume 61, Issue 7, July 2013.

[14] Zhi Hao Jiang, Micah D. Gregory, Douglas H. Werner, "Design and Experimental Investigation of a Compact Circularly Polarized Integrated Filtering Antenna for Wearable Biotelemetric Devices", IEEE Transactions on Biomedical Circuits and Systems, pp. 328-338, Volume 10, Issue 2, April 2016.

[15] M. Klemm, I. Locher, G. Troster, "A novel circularly polarized textile antenna for wearable applications", 7th European Conference on Wireless Technology, pp. 285-288, Oct. 2004, Amsterdam.

[16] Zhi Hao Jiang, Douglas H. Werner, "A Compact, Wideband Circularly Polarized Co-Designed Filtering Antenna and Its Application for Wearable Devices with Low SAR", IEEE Transactions on Antennas and Propagation, pp. 3808 – 3818, Volume 63, Issue 9, Sept. 2015.

[17] Kyohei Yamaguchi, Kuniaki Yoshitomi, Haruichi Kanaya, "Development of 5GHz Circularly Polarized Slot Antenna", 2016 IEEE 5th Asia-Pacific Conference on Antennas and Propagation (APCAP), pp. 59-60, July 2016, Kaohsiung.

[18] Computer Simulation Technology, ver. Studio 2016, online: https://www.cst.com/2016.

[19] Less EMF. Inc, online: https://www.lessemf.com.